PROCEEDINGS OF SPIE

SPIEDigitalLibrary.org/conference-proceedings-of-spie

Normalized difference indices in Landsat 5 TM satellite data

M. Delgadillo-Herrera, M. Arreola-Esquivel, C. Toxqui-Quitl, A. Padilla-Vivanco

M. Delgadillo-Herrera, M. Arreola-Esquivel, C. Toxqui-Quitl, A. Padilla-Vivanco, "Normalized difference indices in Landsat 5 TM satellite data," Proc. SPIE 11104, Current Developments in Lens Design and Optical Engineering XX, 111040W (30 August 2019); doi: 10.1117/12.2532322

Event: SPIE Optical Engineering + Applications, 2019, San Diego, California, United States

Normalized difference indices in Landsat 5 TM satellite data

M. Delgadillo-Herrera, M. Arreola-Esquivel, C. Toxqui-Quitl, and A. Padilla-Vivanco

Computer Vision Laboratory, Universidad Politécnica de Tulancingo, Hgo. 43629, México

ABSTRACT

Urban growth, deforestation, water resources and thawing of the poles due to globe worming are topics of interest in the research community. Normalize difference indices are utilized in remote sensing to analyzed and classify surface cover types. In this paper research, a multispectral satellite data from Landsat 5 TM is preprocessing, in order to addresses and evaluates accuracy of Normalized difference Built-up Index (NDBI), Normalized Difference Vegetation Index (NDVI), Automated Water Extraction Index (AWEI) and Normalized Difference Snow Index (NDSI) at different time scenes. A quantitative statistical pixel percentages of build-up, vegetation cover, snow/ice and water body is given in this study for different periods of time.

Keywords: Landsat 5 TM, Remote sensing, radiometric correction, NDVI, AWEI, NDBI, NDSI.

1. INTRODUCTION

The sustainability of natural resources is an important issue for the development of future generations and social welfare throughout the world. The scientific community dedicates time and effort to understand, measure and quantitatively predict the ecological effects due to deforestation, thawing of the poles, the lack of fresh water, the urban population, among others [1, 2]. Long-term Landsat data allows remote sensing of the earth-environmental change over time. Since Landsat 5 TM was launched in March 1984 by the National Aeronautics and Space Administration (NASA) and decommissioned in January 2013, it is an invaluable resource for the temporal and spatial analysis of vegetation, water, snow and build-up areas [3]. Several multi-band index approaches have been introduced in the literature to delimit these areas in which advantages and disadvantages of discriminating certain materials from others stand out. In this research paper we analyze the multi-band index basic principles (spectral signature in significant units) that were taken into account to increase the intensity contrast of the Region Of Interest (ROI) and the background. The Normalized difference Built-up Index (NDBI), Normalized Difference Vegetation Index (NDVI), Automated Water Extraction Index (AWEI) and Normalized Difference Snow Index (NDSI) are compute at different date and time using Landsat 5 TM multispectral images. In Table 1 is shown the wavelength bands and spatial resolution.

Table 1. Band specifications of Landsat 5 TM [4].

BANDS	**Landsat 5 TM**	
	Wavelength (μm)	**Spatial resolution** (m)
Band 1 (Blue)	0.45 - 0.52	30
Band 2 (Green)	0.52 - 0.60	30
Band 3 (Red)	0.63 - 0.69	30
Band 4 (NIR)	0.76 - 0.90	30
Band 5 (SWIR-1)	1.55 - 1.75	30
Band 7 (SWIR-2)	2.08 - 2.35	30

Before performing any ecological analysis or earth-surface mapping, the multi-temporal Landsat 5 TM imagery must be preprocessed. Multispectral image-distortion is a common effect in multi-temporal satellite data due to the difference in solar angle, sensor degradation, scattering and atmospheric absorption. The preprocessing steps allow to obtain similar atmospheric conditions in multi-temporal spectral images to deliver high quality data results [5]. The workflow of this document is as follows: In Section 2, the mathematical methods for normalized difference indices and spectral profiles are shown. In Section 3, outlines the indices extraction results. Finally in Section 4, a main conclusion is given.

Current Developments in Lens Design and Optical Engineering XX, edited by R. Barry Johnson,
Virendra N. Mahajan, Simon Thibault, Proc. of SPIE Vol. 11104, 111040W · © 2019 SPIE
CCC code: 0277-786X/19/$21 · doi: 10.1117/12.2532322

2. INDEX BASED METHODS IN SATELLITE DATA

In order to analyze a geographical environment over time by means of satellite images, it is necessary to pre-process the data. The geometric corrections, solar correction and atmospheric correction were done using ENVI version 5.1 (Exelis Visual Information Solutions, Boulder, Colorado). The index-based methods definition for vegetation, water, snow and built-up are analyzed below.

2.1 Normalized Difference Vegetation Index (NDVI)

The spectral profile can be used for the identification of materials, where is plotted the wavelength (spectral bands) versus the percentage of reflectance (ratio between ascending and descending radiation). Figure 1 (a) shows the selected pixel belonging to the vegetation in six spectral bands of the Landsat 5 TM satellite data. In the Figure 1 (b) the spectral signature of the selected vegetation pixel is observed, showing a greater reflectivity in the near infrared (NIR). Also, displaying low reflectance in the visible (blue, green and red) and shortwave infrared (SWIR).

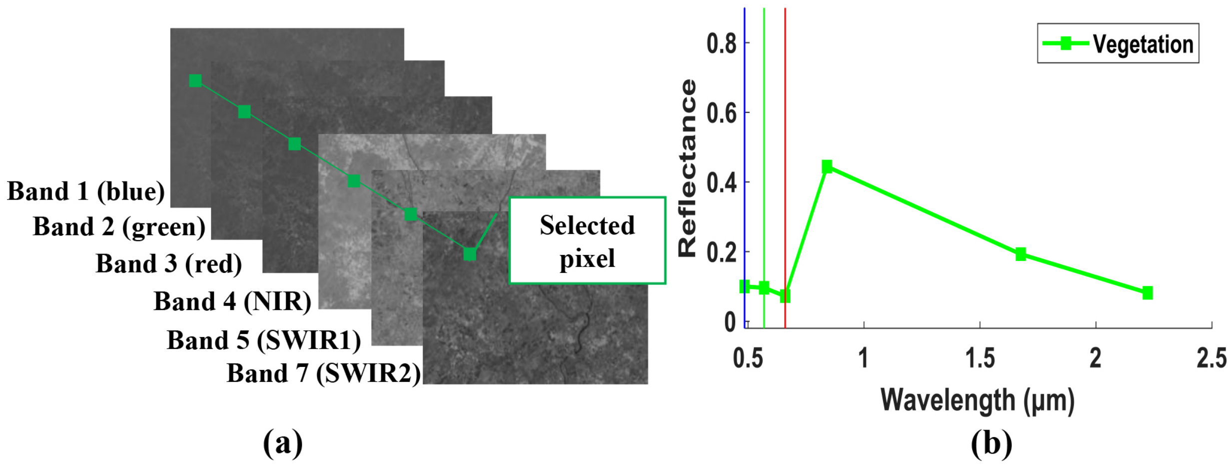

Figure 1. (a) Selection of a pixel belonging to vegetation in six spectral bands of Landsat 5 TM, and (b) spectral signature of the vegetation pixel.

The earliest study using the Normalized Difference Vegetation Index (NDVI) was by Rouse [6] in 1973 and later by Tucker [7] in 1981. The purpose is maximize the high reflectance by the NIR band and minimize the low reflectance of the red that produces the vegetation by its characteristics. The NDVI can be calculated by the following expression,

$$NDVI = \frac{(Band4 - Band3)}{(Band4 + Band3)}, \tag{1}$$

where Band 3 y Band 4 are spectral bands that belong to the Landsat 5 TM satellite shown in Table 1.

2.2 Automated Water Extraction Index $AWEI_{nsh}$ no shadows

Based on the water spectral analysis different water bodies extraction indexes have been developed in the literature, with the purpose of increasing the intensity contrast of the pixels belonging to the region of interest (water) from the background pixels (vegetation, buid-up, soil, among others). Figure 2 (a) shows the selected pixel belonging to water extracted in 6 spectral bands. Figure 2 (b) shows the spectral signature of the selected water pixel, it is observed a greater reflectivity in the visible portion (blue, green and red) and low reflectance in the NIR and SWIR ranges.

Among the techniques for the extraction of water bodies, the Automated Water Extraction Index no shadows proposed by Feyisa [8] stands out, to separate pixels belonging to water from pixels belonging to other types of

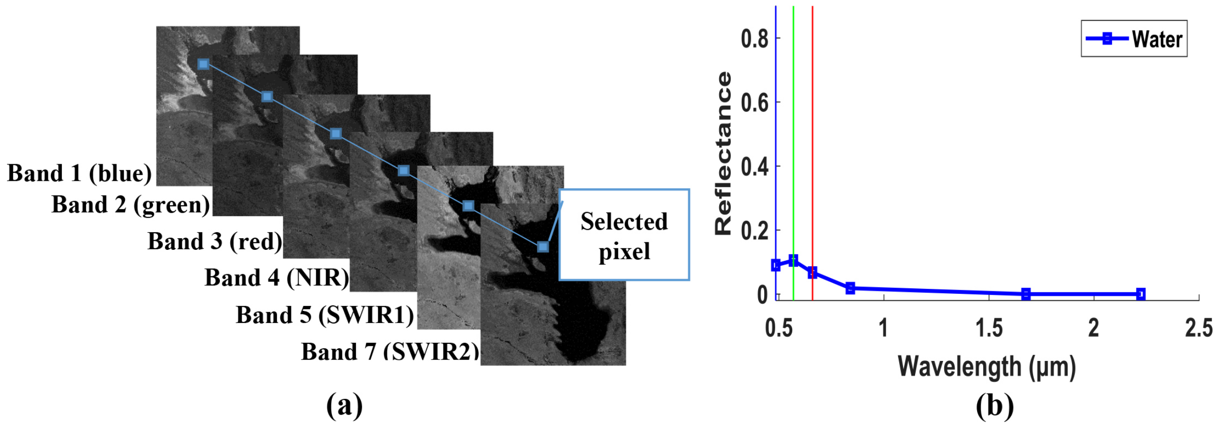

Figure 2. (a) Selection of a pixel belonging to water in six spectral bands of Landsat 5 TM, and (b) spectral signature of the water pixel.

surfaces. For the formulation of $AWEI_{nsh}$ an arithmetic combination of five multispectral bands are used to define as,

$$AWEI_{nsh} = 4(R_{Band2} - R_{Band5}) - (0.25R_{Band4} + 2.75R_{Band7})\,, \tag{2}$$

where R is the reflectance value of the Band 2, Band 4, Band 5 and Band 7 shown in Table 1.

2.3 Normalized Difference Snow Index (NDSI)

Figure 3 (a), shows the selected pixel belonging to snow/ice in six spectral bands. The spectral profile of snow/ice can be seen in Figure 3 (b), it shows greater reflectance in the range of the visible and near infrared, meanwhile, decaying in the short wavelengths.

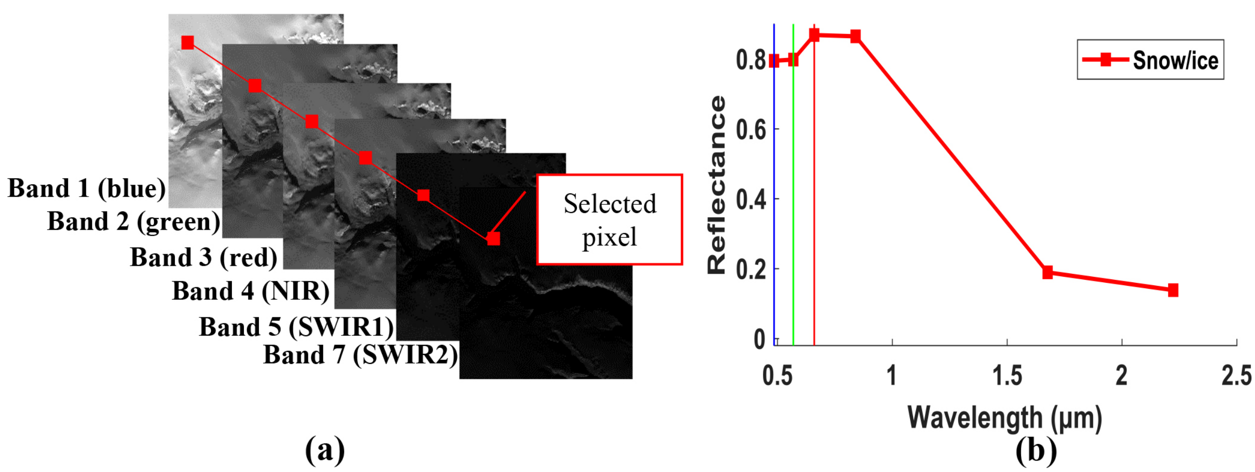

Figure 3. (a) Snow/ice pixel selection in six spectral bands of Landsat 5 TM, and (b) spectral signature of snow/ice pixel.

To identify snow, Hall [9] introduced the Normalized Difference Snow Index (NDSI) in 1995, based on the fact that snow reflects mostly in visible light and absorbs radiation at infrared wavelengths. For the NDSI formulation, two spectral bands belonging to the Landsat 5 TM satellite can be used as,

$$NDSI = \frac{(Band2 - Band5)}{(Band2 + Band5)}\,, \tag{3}$$

where, Band 2 and Band 5 specifications are shown in Table 1.

2.4 Normalized difference Built-up Index (NDBI)

To obtain the spectral signature a selected pixel belonging to a built area is used. In the build-up spectral profile of the Figure 4 (b), a low reflectance is observed in the wavelength range of the visible. While, the maximum reflectance is shown in the NIR and (SWIR) wavelength range.

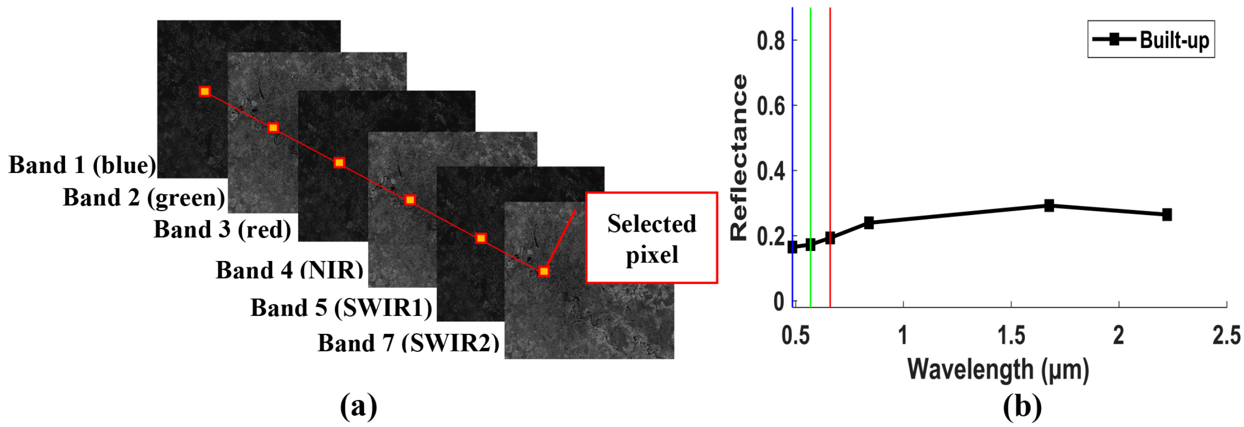

Figure 4. (a) Selected pixel in TM reflectances for built-up area, and (b) spectral profile of built-up pixel.

The Normalized difference Built-up Index (NDBI) proposed by Zha [10] in 2003 to extract urban surfaces, is defined as,

$$NDBI = \frac{Band5 - Band4}{Band5 + Band4}, \tag{4}$$

where, Band 4 and Band 5 wavelength characteristics are shown in Table 1. The NIR and SWIR wavelengths are used in this formulation to obtained negative pixel values for water bodies and positive numbers for built-up.

3. INDEX EXTRACTION RESULTS

In this paper results, the Normalized difference indices are used to analyze environmental change detection using the long-term Landsat 5 TM data. Vegetation cover, urban areas, water bodies and snow cover may suffer significant alterations over time. These environmental variation provide information that can be analyzed for better future decision making.

3.1 Automated Water Extraction Index $AWEI_{nsh}$ no shadows

Lake Poopó is located in Bolivia with a latitude of $-18.806288°$ S and longitude of $-67.095296°$ W. The Figure 5 shows $AWEI_{nsh}$ results for different years in sub-images with a dimension of 1911x2959 pixels. It can be observed that Lake Poopó is drying up through the years. With a decreasing percentage water pixel value presented in Table 2. The total percentage of water is calculated from the binarized $AWEI_{nsh}$ images of Figure 5g-5i.

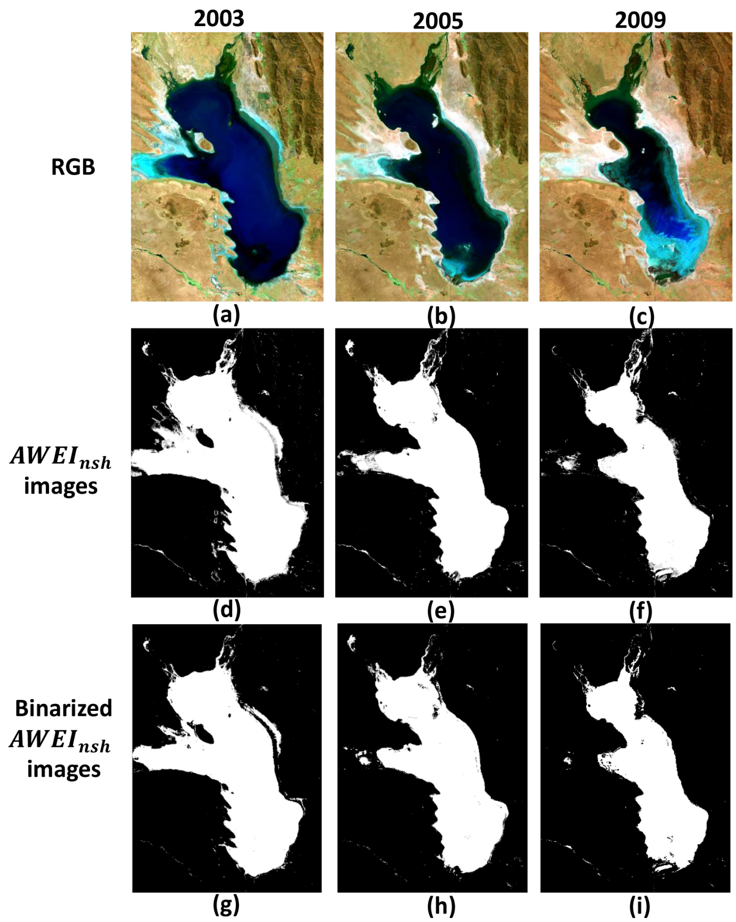

Figure 5. Lake Poopó in August 2003, 2005 and 2009. (a), (b) and (c) RGB Landsat mosaic using Band 7, Band 4 and Band 2. Imageries (d), (e) and (f) are non-binarized $AWEI_{nsh}$ and (g), (h), (i) are binarized $AWEI_{nsh}$ images mapping surface with threshold number = 1.20829.

Table 2. Water pixels percentages of Bolivia binarized images given by ENVI.

2003	**2005**	**2009**
30.501142%	25.030619%	19.835817%

3.2 Normalized Difference Vegetation Index (NDVI)

Spain region with a latitude of 43.100691° N and longitude of −7.650026° W is observed in Figure 6. The NDVI result for sub-images of size $320x232$ pixels shows a low plant density in April 1984, increasing in 2005 and a higher plant density in April 2009. This increase can be confirmed in Table 3 , which illustrates the amount in percentage of vegetation coverage. The total percentage of vegetation is calculated from the binarized NDVI images of Figure 6g-6i.

Table 3. Total percentage of vegetation pixels in binarized images of the Spain region given by ENVI software.

1984	**2005**	**2009**
12.680496%	21.672953%	23.624731%

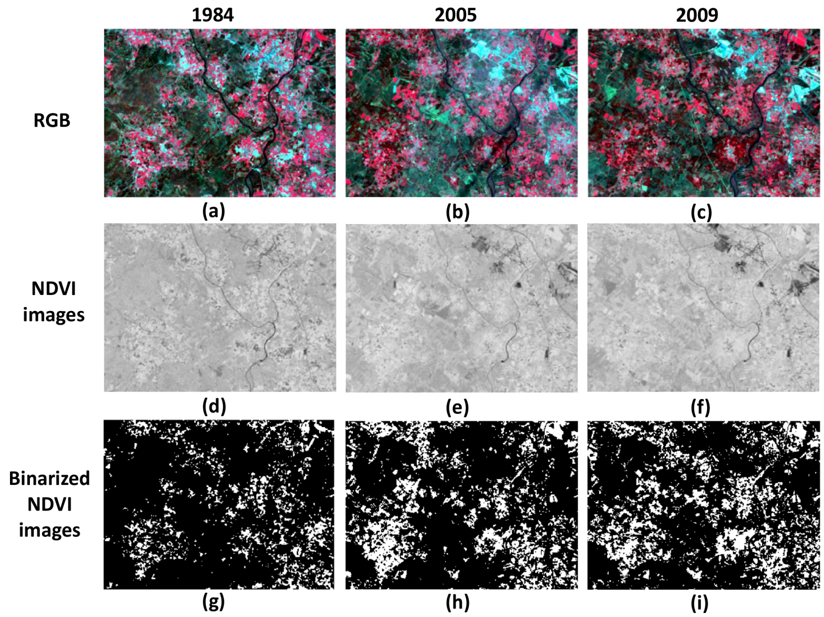

Figure 6. Region of Spain in April 1984, 2005 and 2009. (a), (b) and (c) are RGB images using the Band 4, Band 3 and Band 2. The vegetation is shown in red color since it reflects light in the NIR band. Images (d), (e) and (f) are non-binarized $NDVI$ results and (g), (h), (i) are $NDVI$ with threshold number = 0.59693.

3.3 Normalized Difference Snow Index (NDSI)

The center of the study area of Greenland is located at latitude $73.8603° \ N$ and longitude $-22.7857° \ W$. The dimension of the sub-images are $961x629$ pixels presented in Figure 7. The delineation snow cover using the NDSI method shows a snow melting through time. Moreover, Table 4 shows a statistical decrease in the total number of snow pixels in the Greenland region. The total percentage amount of snow is calculated from the binarized NDSI images of Figure 7g-7i.

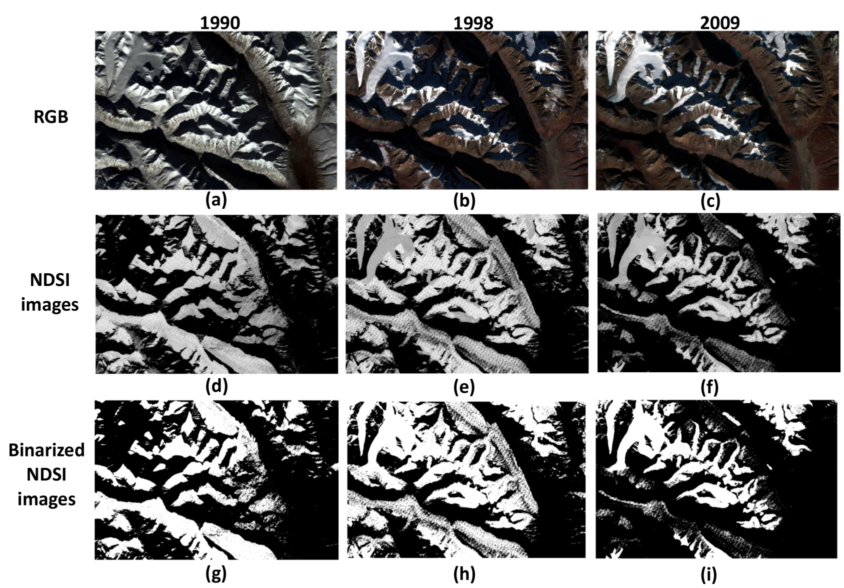

Figure 7. Greenland region registered in September 1990, 1998 and 2009. (a), (b) and (c) The ROI RGB images. Imageries (d), (e) and (f) are Non-binarized $NDSI$ and (g), (h), (i) are $NDSI$ results with threshold number = 0.24893.

Table 4. Percentage variation of snow pixels in Greenland region, given by ENVI.

1990	1998	2009
31.899568%	44.103006%	24.343846%

3.4 Normalized difference Built-up Index (NDBI)

The delimitation of the built-up areas in the Moscow city with a latitude 55.731138° N and longitude of 37.611004° E is shown in Figure 8. The size of the sub-images is 3601x3601 pixels. A visually inspection indicates a growth in urban land cover from 1996 to 2011. Also, quantitatively the increment of the amount of built-up pixels can be seen in Table 5. The total percentage amount of built-up is calculated from the binarized NDBI images of Figure 8g-8i.

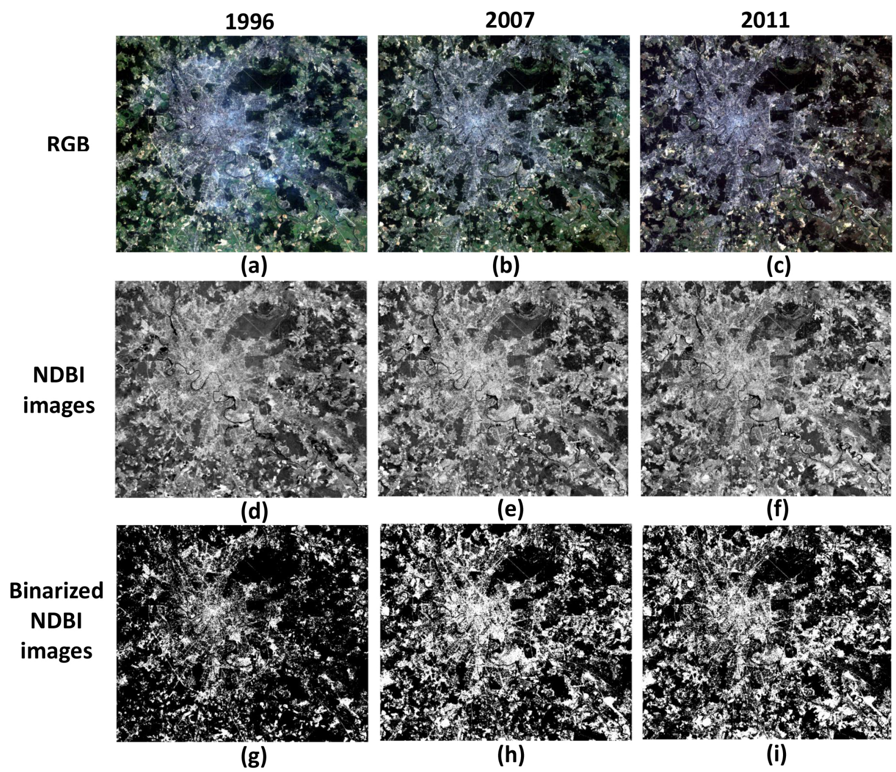

Figure 8. Moscow city in August 1996, 2007 and 2011. (a). (b) and (c) RGB images of the region of interest. Images (d), (e) and (f) are non-binarized built-up extractions and (g), (h), (i) are $NDBI$ with threshold number = -0.13894.

Table 5. Built-up pixels percentages in Moscow binarized images, given by ENVI.

1996	2007	2011
21.29826%	35.392304%	36.152817%

4. CONCLUSIONS

Due to the difference of the zenith angle, the degradation that the sensor suffers through time, the absorption and the dispersion among other aspects, it is necessary to perform the radiometric calibration and appropriate atmospheric correction.The correct preprocessing steps deliver comparable scenes and high quality data in different date and time.

The normalized difference indices are simple arithmetic combination of multispectral bands, which does not require a high computational cost to obtain satisfactory results. The unique spectral signature of certain materials can have a similar reflectance in a single wavelength but differs in others. Based on the normalized difference of the low and high spectral reflectance, the muti-band methods enhance the separation between the study surface from the background in a single or multiple scenes.

The monitoring of environmental surface change has been observed in diverse study areas at different periods of time. In the Figure 5g-5i, an increasing vegetation pixel percentage range of [12.680496%, 23.624731%] is obtained from 1984 to 2009. This variation is related to the increasing amount of plant density in the selected region. A statistical percentage range of [31.899568%, 24.343846%] for a decreasing snow cover is obtained from Figure 6g-6i by means of NDSI analysis. The NDBI binarized images from Figure 7g-7i, an urban area growth is observed in Moscow city in the period between August 1996 to August 2011. From 8g-8i binarized AWEI results, a decreasing water pixel percentage range of [30.501142%, 19.835817%] is obtained. This decreasing, is associated to the declining amount of water that the Lake Poopó have been loss through the years.

ACKNOWLEDGMENTS

M. Delgadillo-Herrera and M. Arreola-Esquivel thank to Consejo Nacional de Ciencia y Tecnología (CONACyT); with CVU no. 858588 and 858585. We thank the support of PADES program; Award no. 2018-13-011-047. And we thank to Politecnico di Torino by the support during the research stay in October-November 2018 and May-June 2019.

REFERENCES

[1] Ottinger, M., Kuenzer, C., Liu, G., Wang, S., and Dech, S., "Monitoring land cover dynamics in the yellow river delta from 1995 to 2010 based on landsat 5 tm," *Applied Geography* **44**, 53–68 (2013).

[2] Valdiviezo-N, J. C., Castro, R., Cristóbal, G., and Carbone, A., "Hurst exponent for fractal characterization of landsat images," in [*Remote sensing and modeling of ecosystems for sustainability Xi*], **9221**, 922103, International Society for Optics and Photonics (2014).

[3] USGS, "What are the band designations for the Landsat satellites?." USGS, 2018 https://www.usgs.gov/faqs/what-are-band-designations-landsat-satellites?qt-news_science_products=0#qt-news_science_products. (Accessed: 15 December 2018).

[4] USGS, "Landsat Missions." USGS, 2018 https://www.usgs.gov/land-resources/nli/landsat/landsat-5?qt-science_support_page_related_con=0#qt-science_support_page_related_con. (Accessed: 16 September 2018).

[5] Young, N. E., Anderson, R. S., Chignell, S. M., Vorster, A. G., Lawrence, R., and Evangelista, P. H., "A survival guide to landsat preprocessing," *Ecology* **98**(4), 920–932 (2017).

[6] Rouse Jr, J., Haas, R., Schell, J., and Deering, D., "Monitoring vegetation systems in the great plains with erts," (1974).

[7] Tucker, C. J., Holben, B. N., Elgin Jr, J. H., and McMurtrey III, J. E., "Remote sensing of total dry-matter accumulation in winter wheat," *Remote Sensing of Environment* **11**, 171–189 (1981).

[8] Feyisa, G. L., Meilby, H., Fensholt, R., and Proud, S. R., "Automated water extraction index: A new technique for surface water mapping using landsat imagery," *Remote Sensing of Environment* **140**, 23–35 (2014).

[9] Hall, D. K., Riggs, G. A., and Salomonson, V. V., "Development of methods for mapping global snow cover using moderate resolution imaging spectroradiometer data," *Remote sensing of Environment* **54**(2), 127–140 (1995).

[10] Zha, Y., Gao, J., and Ni, S., "Use of normalized difference built-up index in automatically mapping urban areas from tm imagery," *International journal of remote sensing* **24**(3), 583–594 (2003).